

# Monte Carlo Simulation of Flow in Three-Dimensional Discrete Fracture Networks

**H. Mustapha**

Applied Mathematics Department, University of Maine  
Le Mans 72000, France ; Tel: (+33) 6 70 38 72 89.  
E-mail: Hussein.Mustapha@univ-lemans.fr

**Abstract.** The normal fractured mediums are strongly unforeseeable because of the existing complex structures on the scale of the fracture and the scale of the network. Numerical modeling can provide significant information on underground phenomena of flow. However the structure of network is difficult for generating a grid mesh and has like consequence of the very great fields to simulate. In the works [1,2], we presented a new approach to simplify the existing complex configurations in the fracture networks. First, we showed the good quality of the grid mesh obtained by using a projection method. In second step, we validated the proposed approach and compared between the approximate solution and a reference solution. In this article, the reference solution is calculated using the projection method and finest mesh. After, we vary the step of mesh to establish a relation between the error and the precision of the solution on one hand and the cost of calculation on the other hand. To conclude, the projection method represents an adaptive method of the complex configurations.

**Keywords:** Darcy flow, stochastic discrete fracture network, Monte Carlo simulation, Mixed-hybrid finite element method, projection method.

## 1. Introduction

The underground waste repository projects and exploitation of hot, dry, rock geothermal energy have spurred studies in fracture networks transport properties. Many site-specific studies have flourished around various projects [3], which are generally based on a careful characterization of the structure of the fractured rock mass, with the classical difficulty of deducing three-dimensional information from one- or two-dimensional field data [4]. Then the hydraulic properties are computed by using reconstructed model networks, based on the experimental geometrical characteristics, and various flow models. The fluid flow modeling in the underground media requires considering their very high geological heterogeneity. The complexity of the geological mediums comes from the metamorphic and sedimentary processes, and mechanics which create structures having hydraulic properties varying in several orders of magnitude and correlated over a broad range of scales. In the fractured mediums, of matrix of very low permeability, the flow of the fluid is focused in the highly heterogeneous fractures [5]. The objective of numerical modelling initially consists in simulating hydraulic phenomena in a great number of networks containing a great number of fractures, i.e. from  $10^3$  to  $10^5$ , and in the second time to seek an optimum between the quality of the approximation of hydraulic simulation on one hand and the costs (computing time and the memory capacity) on the

other. In Figure 1, we present a very complex discrete fracture network (FN) [6,7,8]. This network contains difficult configurations that complicate the generation of the fractures mesh. Their number and their difficulty increase with the number of the fractures generated. These configurations are found as well in the stochastic generation of the natural environments fracture networks.

The major purpose of the present paper is to develop a full solution of the steady flow problem in a general three-dimensional complex network made of two-dimensional ellipse fractures as illustrated in Figure 1. A literature survey shows that in most cases, the description is two dimensional [9] or that the three-dimensional network is replaced by a capillary model. The intersection of two fractures is schematized by a channel that joins their centers with an effective hydraulic conductivity that results from simple geometric arguments; this model is improved in [3,10,11] by introducing flow channels in the fractures, which results in complex capillary networks. *Nordqvist et al.* [12] went one step further by building the network from a library of fractures with spatially variable apertures for which flow was solved beforehand. However, again, the final representation is a tube model. These capillary models suffer two main flaws. First, the assignment of the bond conductivities is somewhat arbitrary and the assumption that the fluid flows from center to center is unrealistic. Second, only pair intersections are taken into account. Another method is the boundary element method [4], the solution is correctly computed in the plans of the fractures. This method is limited to the homogeneous fractures and the fracture networks treated contain a very limited number of fractures [13,14]. *Mariska and Vobralik* [15,16] develop a new method based in the simplification of complex configurations. In there works, the approximate solution computed using the developed approach is not validated. Finally, we don't have any idea about the precision error using this type of simplifications. To conclude, the general limits of these methods are obtained from the limited number of fractures, and the taking into account only of a part of natural networks complexity.

In our numerical approach, developed in [1,2], we consist to project the fractures in 3D regular grid. We have showed that the approximate solution is very precise and very close to the reference solution computed using finest mesh. In this paper we study the loss in precision induced using the projection method and the mesh quality obtained by varying the mesh step. After, we observe the evolution of the memory capacity and the CPU time for the same variation of mesh step. This paper is organized as follows: First, we present quickly the mathematical model and the numerical method used to discretize the Darcy law. In the second step, we present numerical examples to demonstrate the efficiency and robustness of our numerical approach. Finally, a summary and a preview of future work are presented.

## 2. Mathematical model

We define the fracture network  $R$  by  $R \equiv \{ \bigcup_{i=1, n^F} \overline{F_i} \setminus \partial R \}$ , where  $F_i$  is the fracture  $i$  (modeled by ellipse),  $n^F$  is the number of fractures and  $\partial R$  is the network boundaries. We seek the fracture flow velocity  $u$  (a two-dimensional vector in each  $F_i$ ), which is the solution of the problem:

$$u = -K(\nabla p + \nabla z) \quad \text{in } R \quad (1a)$$

$$\nabla \cdot (u) = F \quad \text{in } R \quad (1b)$$

$$\begin{aligned} p &= p_D && \text{on } \Gamma_D \\ u \cdot n &= u_N && \text{on } \Gamma_N \end{aligned} \quad (1c)$$

where all the variables are expressed in the local coordinates of appropriate  $F_i$  and the differentiation is always done with respect to these local coordinates. Eq. (1a) is Darcy's law, (1b) is the mass balance equation, and (1c) prescribes Dirichlet and Neumann boundary conditions. The variable  $\mathbf{p}$  denotes the piezometric head,  $\mathbf{p} = \bar{p} / \rho g$ , where  $\bar{p}$  is the fluid pressure,  $g$  is the gravitational acceleration constant,  $\rho$  is the fluid density,  $f$  represents stationary sources or sinks density, and  $z$  is the elevation, i.e. the upward vertical three-dimensional coordinate. The second-rank tensor  $K$  of hydraulic conductivity is a function of the original three-dimensional fracture aperture, wall roughness, and filling. We suppose that  $K$  is symmetric and uniformly positive definite on each  $F_i$ .

### 3. Numerical method in fracture network

The numerical approach used to solve the system of Eqs. (1a-1c) is based on the mixed hybrid finite element (MHFE) method. We consider a spatial triangulation of the computational domain  $R$  consisting of triangles or quadrilaterals. Unlike some other numerical methods, no restrictions are imposed on the element geometrical shape. The essential idea of the MHFE method is to approximate simultaneously the pressure and its gradient. The velocity field is approximated in the so-called Raviart-Thomas space of lowest order (RT0) (see, e.g., [17,18,19]). The main idea is to express the velocity over each grid cell with respect to the fluxes across the cell edges. Different aspects of the numerical approach, the discretization of Darcy's law by the mixed-hybrid finite element method are discussed in detail in [1,2]. The triangulation of the fracture network is obtained by discretization of each fracture into a triangular mesh respecting the intersections with other fractures. In order to decrease the number of elements and to avoid ill-conditioned matrices resulting from the cases where there exist elements with very small angles, the algorithm should in addition simplify the geometrical situation. To simplify the complex configurations of the fractures, we projected the boundaries of fractures and the intersections on three-dimensional regular grid (3DRG). The developed method offers a regular base to generate, with a good quality, the triangulation mesh of the fractures. Therefore, we do not need more to refine the triangulation mesh to improve the quality. Otherwise, we can generate the triangulation for all fracture networks presenting complex configurations. As an example, of triangulation mesh and computing solution, see the Figure 2. For more details, we refer to [1,2].

### 4. Numerical experiment

In [1,2], we validated the approximate solution using the projection method. We showed that by working with a finest mesh, the proposed approach gives a very precise solution. Then, this very interesting result helps to study the very complex fracture networks. In fact, because of complex configurations of fracture network, the triangulation of this network is in most cases impossible.

To conclude, the projected method can give a reference solution (working in finest mesh) for all complex fracture networks. In this section, we measure the precision error by varying ( $h$ ). First, we evaluate the errors in global equivalent permeability, the flow across each fracture and each intersection. After, we observe the mesh quality obtained; we compute the linear system size and the memory capacity for each step  $h$ . To fix the idea, we consider in the following that the approximate solution obtained using the projection method in finest regular grid, as a reference solution.

## **Test 1: simulation in one fracture network**

In this test, we simulate the flow in the fracture network  $FN$  (Figure 1). For this network we compute some solutions computed for different values of  $h$ . The aim is to observe the evolution of precision error, the mesh quality and the improvement in CPU time and memory capacity with respect to  $h$ .

### **1. Mesh quality**

In Figure 3, we present the curves that represent the mesh quality of the network ( $FN$ ) for each mesh step. This figure shows that the majority of mesh triangles angles is near to  $60^\circ$ . Then, we deduce that the mesh quality remains very good by varying the mesh step. This result is interesting because it is necessary to have a good quality mesh to compute correctly all solutions by reducing the problem size at same time.

### **2. Precision error**

For each step  $h$ , we calculate the differences between the approximate solution and the reference solution calculated while projecting on a finest grid (Figure 4). The difference between the approximate solution and the reference solution remains always weak. We can conclude that the solution calculated by increasing the step mesh remains precise. We carry out a linear regression to consider the error corresponding to the equivalent permeability. According to what precedes, the straight regression lines represent more than 98% of the distribution of the points and the data are well estimated. This result is coherent with the numerical estimate error of the MHFE method which is  $O(h)$  (method of order 1). We checked in the two preceding parts that the approximate solution obtained with the projection method makes it possible to consider rather large steps of mesh.

### **3. Improvement in CPU time and memory capacity**

The projection method provides an improvement in CPU time and memory capacity by decreasing the size of problem. The more the step of mesh is large, the better is the improvements of CPU time and memory capacity (Table 1). For one variation of  $h$  between 0.08 and 0.21 the linear system size (resp. the memory mesh and the nonzero elements of  $A$ ) decreases from 313 776 to 50 588 (resp. from 1 882 656 to 303 528 and from  $1.58 \times 10^6$  to  $0.26 \times 10^6$  real values to storage). To conclude, the decrease of memory capacity needed is of 85%. However, the decrease of the linear system size reduces the time of the linear system resolution. The obtained result (Table 2) shows that the CPU time decreases from 28 seconds to 2.5 seconds, using the direct linear solver *umfpack* [20]. To conclude the improvement in CPU time is equal to 92%.

## **Test 2: Monte Carlo simulation**

The characteristics of fractures are generated stochastically. The orientation, the length, the position and the eccentricity of the fractures are generated according to statistical laws. To generate a network of fractures, we fix the type of distributions and the seeds. For the same parameters distributions, we can generate a great number of networks by changing the seeds. In this part, we choose a set of parameters distributions (SD) (Figure 3). We generate 70 networks for SD by changing the seeds and fixing the exponent of the power law, the cube size, and the minimal length of a fracture and the density of the fractures (a threshold density). To fix the ideas, we note by  $GN$  the set of  $NN$  ( $NN$ :

number of networks) networks generated with the distributions  $SD$ . After, we compute the references solutions represented by the average equivalent permeability reference ( $K_{ref}$ ) (e.g., average of the permeabilities computed, on a finest mesh, in the set of networks GN) and the standard deviation ( $\sigma k_{ref}$ ) of this solution. We also seek the average size ( $N_{mref}$ ) of the linear systems associated to the packages of networks and the average time ( $T_{mref}$ ) of resolution of these linear systems and finally, the variations of these values ( $\sigma N_{ref}$  and  $\sigma T_{ref}$ ). The results obtained summed up in Table 4. After the computing of the reference solution, we vary the mesh step  $h$ . The average numerical error for a given value of  $h$  is defined like the difference between the average permeabilities obtained for this step on one hand and the weakest step on the other hand. In this test, we vary  $h$  between 0.02 and 0.2 to observe the variations of the parameters  $N_{mref}$ ,  $T_{mref}$ ,  $K_{ref}$  and of their variations ( $\sigma k_{ref}$ ,  $\sigma N_{ref}$ ,  $\sigma T_{ref}$ ) in the sets of networks  $GN$ . We note by  $T_m$  (resp.  $T_m$  and  $\langle K \rangle$ ) the average time (resp. the average size and the average of equivalent permeability) obtained for each step of mesh and by  $\sigma T_m$ ,  $\sigma N_m$  and  $\sigma k$  the standards deviations. The results obtained appear in Table 5 shows that the error in equivalent permeability, by varying  $h$  from 0.02 to 0.2, is about 7% on one hand and the improvement in CPU time of calculation and in memory capacity are respectively about 96% and 92% on the other hand. These results are very dependent on the value of the parameters and, probably, of deterministic information (e.g., position of the greatest fractures) available on the site. It is foreseeable that the more the quantity of data is significant, the better should be the quality of numerical calculation.

## 5. Conclusion

In this paper, we were interested to validate and study the performance of our approach based on the projection method developed in [1,2]. The validation of the method is carried out in several steps. In [1,2], we initially checked the precision of the approximate solution. In first part, we showed the good quality of the mesh obtained using the projection method. We checked the precision of the solution by comparing it with a reference solution calculated on a finest mesh without projection, in second part. In this paper, we then varied the step of mesh. We showed that the good quality of mesh is preserved. This property is a significant advantage compared to the mesh obtained without projection. We measured the error in precision made during this change of  $h$ , and observed that the algorithm remains of order 1. Finally, we measured the improvement in CPU time and memory capacity and we found that results are very significant and show the efficiency of the numerical approach developed. To conclude, in this paper we showed that the relative error is lower than 7% when  $h$  varies from 0.08 to 0.21, the linear system becomes of six to ten times less large. This reduction in the linear system size induced a reduction of the needed memory, and a significant decrease in CPU times. For example, with a loss of precision lower than 5%, the CPU time and the memory capacity are divided by 10. In forthcoming work, more point can be studied. First, we can make same experiences on different types of fracture networks to study the precision error. On the other hand, we can study other phenomena such as the transient flow, the transport, etc.

## References

1. Mustapha, H. An Adaptive method for Flow Simulation in Three-Dimensional Heterogeneous Discrete Fracture Networks (accepted in the International Conference on Scientific Computing CSC'06, Nevada, USA, June 2006).

2. Mustapha, H., (2005), Simulation numérique de l'écoulement dans des milieux fracturés tridimensionnels. Thèse de Doctorat, *Université de Rennes 1*.
3. Cacas, M.C., and al., (1990), Modeling fracture flow with a stochastic discrete fracture network: calibration and validation. 1. The flow model. *Water Resources Research*, 26, 479.
4. Billaux, D., J.P. Chiles, K. Hestir and J. Long, (1989), Three-dimensional statistical modelling of a fractured rock mass – an example from the Fanay-Augères mine. *Int. J. Rock Mech. Min. Sci. & Geomech. Abstr.*, 26, 281.
5. Neretnieks, I., (1985), Transport in fractured rocks. Proceedings of Hydrogeology of Rock of Low Permeability, *Mem. Intern. Assoc. Hydrogeol.*, 17, 301.
6. Bour, O and P. Davy, (1998), On the connectivity of three dimensional fault networks. *Water Resources Research*, 34, 2611.
7. Bonnet, E., and al., (2001), Scaling of Fracture Systems in Geological Media. *Reviews of Geophysics*, 39, 347.
8. De Dreuzy, J.R., P. Davy and O. Bour, (2000), Percolation threshold of 3D random ellipses with widely-scattered distributions of eccentricity and size. *Physical Review E*, 62, 5948.
9. Rouleau, A. and J.E. Gale, (1987), Stochastic discrete fracture simulation of groundwater flow into an underground excavation in granite, *Int. J. Rock Mech. Min. Sci. & Geomech. Abstr.*, 24, 99.
10. Bruel, D. and F.H. Cornet, (1995), in *Fractured and Jointed Rock Masses*, edited by L.R. Myer, N.G.W. Cook, R.E. Goodman, and C.F. Tsang (Balkema, Rotterdam).
11. D. Billaux, (1990), Hydrogéologie des Milieux Fracturés. Géométrie, Connectivité et Comportement Hydraulique. Thèse de doctorat, *Université d'Orléans*.
12. Nordqvist, A.W. and al., (1992), A Variable Aperture Fractures Network Model for Flow and Transport in Fractured Rocks. *Water Resources Research*, 28, 1703.
13. Dershowitz, W.S. and C. Fidelibus, (1999), Derivation of equivalent pipe networks analogues for three-dimensional discrete fracture networks by the boundary element method. *Water Resources Research*, 35, 2685.
14. Lenti, V. and C. Fidelibus, (2003), A BEM solution of steady-state flow problems in discrete fracture networks with minimization of core storage\*1. *Computers & Geosciences*, 29, 1183.
15. Maryška, J., O. Severýn and M. Vohralík, (2004), Numerical simulation of fracture flow with a mixed-hybrid FEM stochastic discrete fracture network model. *Computational Geosciences*, 8, 217.
16. Vohralik, M., (2004), méthodes numériques pour des équations elliptiques et paraboliques non linéaires: Application à des problèmes d'écoulement en milieux poreux et fracturés. Thèse de Doctorat, *Université Paris XI Orsay*.
17. Raviart, P.A. and J.M. Thomas, (1977), A mixed hybrid finite element method for the second order elliptic problem, *Lectures Notes in Mathematics 606*. Springer-Verlag, New York, 292.
18. Thomas, J., (1977), Sur l'Analyse Numérique des Méthodes d'Elément Finis Hybrides et Mixtes. Thèse de Doctorat d'Etat, *Université de Pierre et Marie Curie*.
19. Hoteit, H. and al., (2002), Numerical Reliability for Mixed Methods Applied to Flow Problems in Porous Media. *Computational Geosciences*, 6, 161.
20. Davis, T.A., (2004), Algorithm 832: UMFPACK, an unsymmetric-pattern multifrontal method with a column pre-ordering strategy. *ACM Trans. Math. Software*, 30(2), 196.

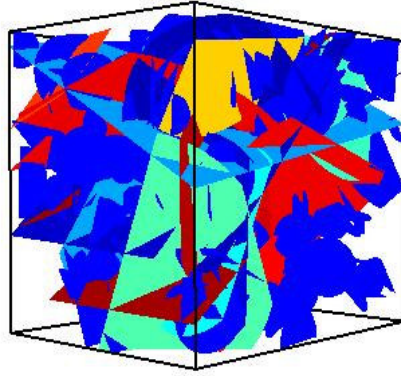


Figure 1. Discrete fracture network (FN). FN contains 500 fractures (modeled by ellipses) generated in a cube of size  $L=8*l_{min}$  where  $l_{min}$  is the minimal size of fracture.

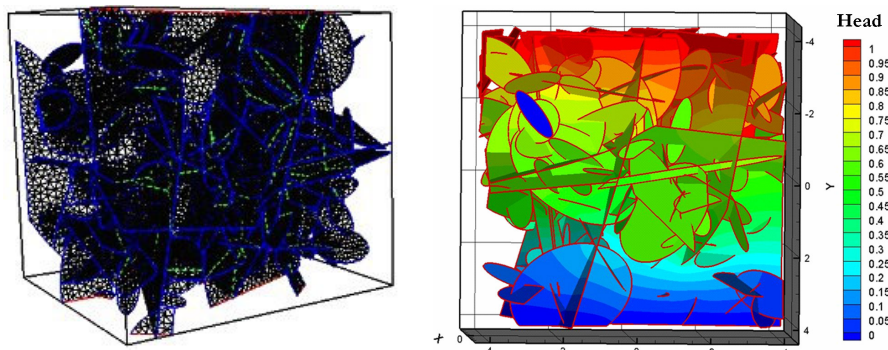


Figure 2. Example of mesh and flow computation of 3D fracture network (left picture: mesh and right picture: flow computation).

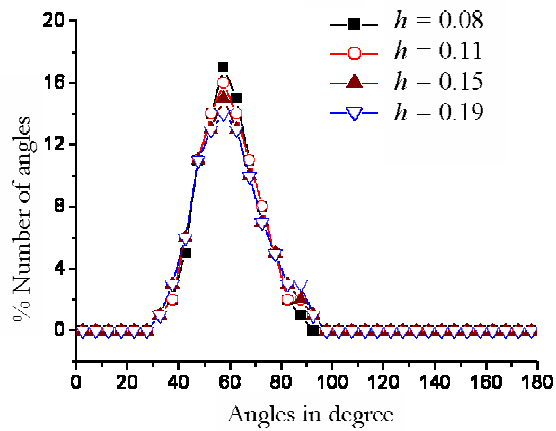


Figure 3. Evolution of the mesh quality of the network FN with the mesh step  $h$ . The obtained mesh obtained with the various steps is of good quality.

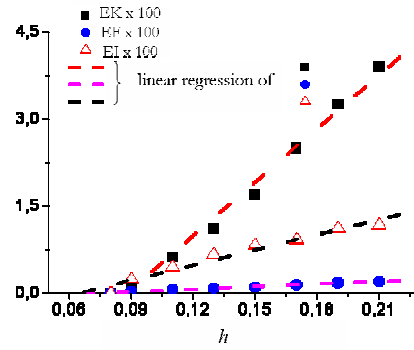


Figure 4. Evolution of the difference expressed as a percentage between the approximate solution and the reference solution. (■) is the relative variation compared to the equivalent permeability, (●) is the variation compared to the average flow of the fractures and (Δ) the variation considering the average flow crossed by the intersections; (---) linear regressions of the data (■), (●), (Δ).

Table 1. Linear system size and memory capacity for various mesh steps.

| $h$  | $SL$    | $MemMesh$ | $nnz(A)$           |
|------|---------|-----------|--------------------|
| 0.08 | 313 776 | 1 882 656 | $1.58 \times 10^6$ |
| 0.21 | 50 588  | 303 528   | $0.26 \times 10^6$ |

Table 2. CPU time corresponding at two different values of  $h$ .

| $h$  | $SL$    | $Time$ |
|------|---------|--------|
| 0.08 | 313 776 | 27.65  |
| 0.21 | 50 588  | 2.36   |

Table 3. Parameters distribution type to generate fracture networks.

| <i>Parameter</i>                | <i>E1</i>                                         |
|---------------------------------|---------------------------------------------------|
| <i>Length of the fractures</i>  | <i>Power Law with exponent <math>a = 3</math></i> |
| <i>Orientation</i>              | <i>Uniform</i>                                    |
| <i>Position</i>                 | <i>Uniform</i>                                    |
| <i>Eccentricity of ellipses</i> | <i>Uniform</i>                                    |

Table 4. Results obtained by simulating the flow in  $GN$  with small value of  $h$ .

|               |           |
|---------------|-----------|
| $h$           | 0.02      |
| $Nmref$       | 1 213 100 |
| $\sigma Nref$ | 350 120   |
| $Tmref$       | 175.3     |
| $\sigma Tref$ | 55.2      |
| $Kref$        | 36.48     |
| $okref$       | 12.23     |

Table 5. Results of simulations in set of networks  $GN$ ;  $Sim$  : simulation.

| $GN$                | $Sim1$           | $Sim3$           | $Sim5$            | $Sim6$           |
|---------------------|------------------|------------------|-------------------|------------------|
| $Dx$                | 0.02             | 0.1              | 0.18              | 0.22             |
| $Nm$                | $1.2 \cdot 10^6$ | $0.4 \cdot 10^6$ | $0.17 \cdot 10^6$ | $0.1 \cdot 10^6$ |
| $\sigma N$          | $3.5 \cdot 10^5$ | $1.3 \cdot 10^5$ | $0.5 \cdot 10^5$  | $0.3 \cdot 10^5$ |
| $Tm$                | 175.3            | 43.45            | 13.16             | 6.9              |
| $\sigma T$          | 55.2             | 22.1             | 6.3               | 3.4              |
| $\langle K \rangle$ | 36.89            | 35.83            | 34.89             | 34.23            |
| $\sigma k$          | 10.1             | 10.2             | 12.23             | 10.45            |